J Therm Anal Calorim (2009) 97:179–183
DOI 10.1007/s10973-009-0242-x

Thermal analysis applied in the crystallization study of $SrSnO_3$

Mary C. F. Alves · Soraia C. Souza · Márcia R. S. Silva · Elaine C. Paris · S. J. G. Lima · R. M. Gomes · E. Longo · A. G. de Souza · Iêda M. Garcia dos Santos

ICTAC2008 Conference

Abstract $SrSnO_3$ was synthesized by the polymeric precursor method with elimination of carbon in oxygen atmosphere at 250 °C for 24 h. The powder precursors were characterized by TG/DTA and high temperature X-ray diffraction (HTXRD). After calcination at 500, 600 and 700 °C for 2 h, samples were evaluated by X-ray diffraction (XRD), infrared spectroscopy (IR) and Rietveld refinement of the XRD patterns for samples calcined at 900, 1,000 and 1,100 °C. During thermal treatment of the powder precursor ester combustion was followed by carbonate decomposition and perovskite crystallization. No phase transition was observed as usually presented in literature for $SrSnO_3$ that had only a rearrangement of SnO_6 polyhedra.

Keywords Stannate · Perovskite · Polymeric precursor method · Pechini · $SrSnO_3$

Introduction

Alkaline earth stannates, with the general formulae $ASnO_3$ and A_2SnO_4 (A = Ca, Sr and Ba) present very interesting properties as recently showed [1–3]. These compounds have been receiving more attention in recent years, as components of ceramic dielectric elements. Strontium stannate, for instance, has been used as humidity sensor [1].

Structure of $SrSnO_3$ is characterized by distorted cubes, due to the inclination of the octahedra. The coordination around Sn^{4+} does not change, as well as the tridimensional arrangement of the octahedra [4]. According to literature data, $SrSnO_3$ undergoes phase transitions, changing from orthorhombic to tetragonal and from tetragonal to cubic, with temperature increase or doping [4, 5].

$SrSnO_3$ has been synthesized by different methods: solid state reaction [3–5] with heat treatment temperature above 1,200 °C, hydrothermal method [2] and polymeric precursor method [6].

The polymeric precursor method, derived from the Pechini is characterized by the formation of a high amount of organic material favoring the formation of carbonates, especially when alkaline-earth elements are present [6–8]. As a consequence, the elimination of this organic material is an important factor which can change the short and long range order.

In this work, $SrSnO_3$ crystallization was evaluated as a function of temperature increase, using thermogravimetry, differential thermal analysis and high temperature X-ray diffraction. Characterization by infrared spectroscopy and X-ray diffraction was also done.

Experimental

The $SrSnO_3$ perovskite was prepared by the polymeric precursor method, as already described in [8]. Tin citrate was the starting material for the synthesis of the $SrSnO_3$.

M. C. F. Alves · S. C. Souza · M. R. S. Silva · E. C. Paris · A. G. de Souza · I. M. Garcia dos Santos (✉)
LACOM, Departamento de Química/CCEN, Universidade Federal da Paraíba, Campus I, João Pessoa, PB, Brazil
e-mail: ieda@quimica.ufpb.br

S. J. G. Lima · R. M. Gomes
LSR, Departamento de Engenharia Mecânica/CT, UFPB, Campus I, João Pessoa, PB 58059-900, Brazil

E. Longo
CMDMC—LIEC, Instituto de Química, UNESP, Araraquara, SP, Brazil

This citrate was obtained using citric acid (99.5%—Cargill) and tin chloride dihydrate (99.9%—Aldrich) [6–8]. A 3:1 citric acid:metal molar ratio was used, besides a 60:40 citric acid:ethylene glycol (99.0%—Vetec) mass ratio.

After de-agglomeration in a 100 mesh sieve, the powder precursors were milled in an atritor mill, in alcohol media, at 500 rpm. After sieving and drying, the precursor was calcined in oxygen atmosphere at 250 °C for 24 h. The thermal characterization of the precursor was performed by thermogravimetry (TG) and differential thermal analysis (DTA), using a TA Instruments—SDT 2960 thermal analyzer. Samples of about 10 mg were heated at 10 °C min^{-1} up to 1,200 °C in air atmosphere with a flow rate of 100 mL min^{-1}, inside alumina pans.

The crystallization of the perovskite phase was evaluated by high temperature X-ray diffraction (HTXRD) that was carried out with Cu-Kα radiation and nickel filter on a SIEMENS D5000 diffractometer equipped with an Edmund Buehler controllable high temperature thermostatic chamber. The heating unit consists of a vacuum heating chamber with a Pt heater, temperature controller to an accuracy of ±1 °C and Pt–PtRh10% thermocouple to monitor the temperature of the sample during the measurements. The heating cycles were performed under ambient atmosphere at a constant heating rate of 40 °C min^{-1} up to the soak temperatures of 500, 600 and 700 °C. Once the temperature reached a constant value the XRD patterns were collected using continuous scanning mode in the 2θ range 40–48° with a scanning speed of 0.02° s^{-1} at a counting time of 2.0 s per step. The total duration of XRD recording was 26.5 min.

The precursor was also calcined with a heating rate of 10 °C min^{-1} up to 300, 400, 500, 600 and 700 °C for 2 h, in air atmosphere. The infrared analyses were carried out in a MB 102 Bomem spectrometer, using KBr pellets, in the range from 4,000 to 400 cm^{-1}. The FT-Raman analyses were done in a FRS/100/S Bruker spectrometer, using Nd:YAG laser, with a power of 60 mW, a wavelength of 1,064 nm, 4 cm^{-1} of resolution, in the range from 10 to 1,200 cm^{-1}.

The sample was also calcined between 900 and 1,100 °C, for characterization using Rietveld refinement of XRD patterns. For these samples XRD data were collected using a Rigaku DMax 2500PC diffractometer applying 40 kV and 150 mA with Cu-Kα radiation, graphite monochromator and rotary anode. In the analysis a 2θ range from 10 up to 110° in a step-scanning mode was used, with step width of 0.02° s^{-1} and fixed time of 3 s. The divergence slit used was fixed at 1° and receiving slit at 0.3 mm. The Rietveld refinement was conducted by means of the (GSAS) package—General Structure Analysis System program of Larson and Von Dreele [9, 10]. The peak profile function was modeled using a convolution of the pseudo-Voigt with the asymmetry function described by Finger et al. [11].

Results and discussion

The TG and DTA curves of the powder precursor are presented in Fig. 1a and b. In TG curves three thermal decomposition steps were observed while DTA curves showed six transitions. At the first step, water and gases adsorbed on the powder surface were eliminated, with an endothermic transition. The second step was assigned to the combustion of the organic material between 300 and 570 °C with exothermic transitions in the DTA curve. Two endothermic transitions were observed in the DTA curves at 650 and 710 °C, with and exothermic peak between them. The last endothermic peak was observed at about 1,091 °C [12].

The elucidation of this behavior was done associating thermal analysis with IR spectroscopy (Fig. 2) and HTXRD (Fig. 3).

In the IR spectra of the sample calcined at 300 °C (Fig. 2), bands were observed at 1630, 1574, 1488_{sh}, 1389, 1088, 850, 770 and 600 cm^{-1}. The band at 1,630 cm^{-1} was assigned to presence of water. Bands at 1,547 and 1,389 were assigned to chelated esters [13]. The intensity of these bands decreased when heat treatment temperature

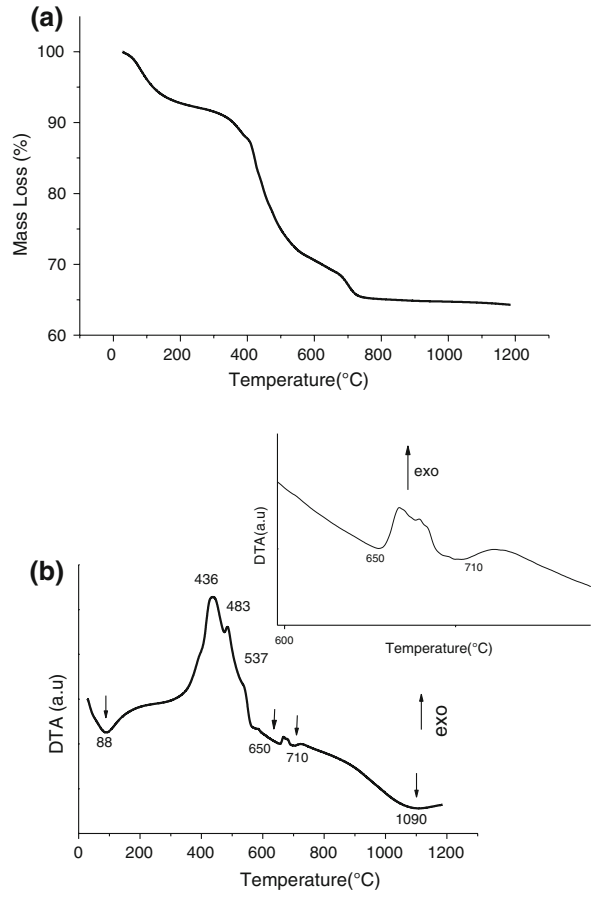

Fig. 1 TG (**a**) and DTA (**b**) curves of the $SrSnO_3$ precursor

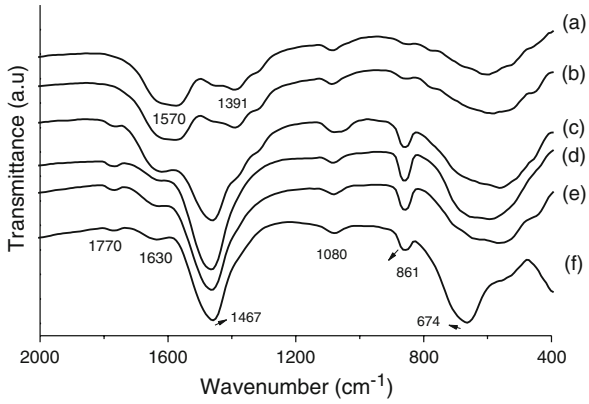

Fig. 2 Infrared spectra of $SrSnO_3$ calcined at different temperatures. (a) 250 °C; (b) 300 °C; (c) 400 °C; (d) 500 °C; (e) 600 °C; (f) 700 °C

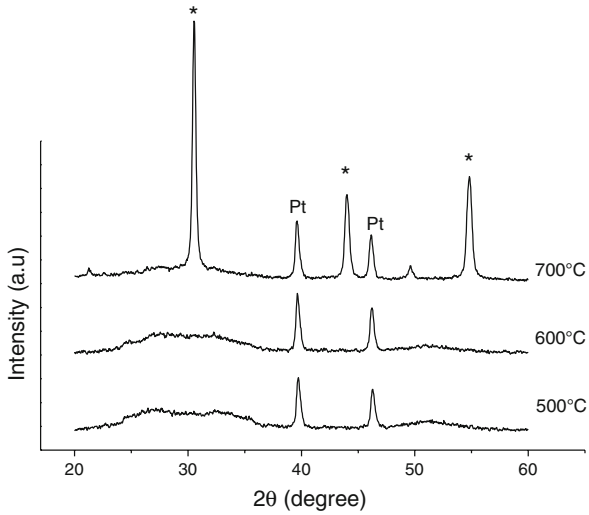

Fig. 3 HTXRD patterns of the $SrSnO_3$, at different temperatures. Legend: *—$SrSnO_3$; Pt—platinum sample holder

increased. These results indicated that the exothermic peaks between 300 and 570 °C were due to the ester combustion.

Bands at 1770, 1488, 1088 and 850 cm^{-1} were assigned to strontium carbonate [13, 14]. The formation of this phase occurred after calcination at 400 °C, increased up to 500 °C and decreased at higher temperatures. Comparing to DTA curve, the endothermic peaks at 650 and 710 °C were assigned to carbonate decomposition.

The vibrations of the stannate group (SnO_3^{2-}) are observed as high intensity bands in the ranges of 300–400 and 600–700 cm^{-1} [15, 16]. The stretching vibration of the Sn–O bond is located at about 530 cm^{-1} [14]. In the present work, these bands were observed at about 674 cm^{-1} with a shoulder at about 535 cm^{-1} and another band starting at about 400 cm^{-1}. The definition of these bands occurred after calcination at 700 °C. This result indicated that the exothermic peaks observed at 668 and 680 °C in DTA curve may be due to the $SrSnO_3$ crystallization.

The HTXRD patterns are presented in Fig. 3. The material was amorphous up to 600 °C and crystalline at 700 °C. This result was in agreement to infrared spectra and indicated that short and long-range ordering occurred simultaneously. It can be concluded that the previous assignment of the exothermic peaks at 668 and 680 °C to perovskite crystallization was correct. These correlations show the importance of the thermal analysis in the understanding of the transformations that occur during the heat treatment of the materials, being also possible to evaluate the crystallization process [12].

Evaluation of the endothermic peak at 1,090 °C was done using Rietveld refinement of the XRD patterns of samples calcined between 900 and 1,100 °C (Fig. 4). The structural parameters and the amounts of the different phases are presented in Tables 1 and 2, respectively. SnO_2 precipitation with cassiterite structure was observed in all samples. $SrCO_3$ was not observed, confirming that the endothermic peak at 710 °C in the DTA curve was correctly assigned to the strontium carbonate decomposition.

Analysis of the refinement index (Table 1) indicated that a good fit was obtained for all calcination temperatures. Except for the χ^2 values, the refinement indexes were maintained in a small variation range and with low values indicating the fit quality. The high values of the χ^2 parameter were due to the secondary phase (SnO_2), which was the only one with relatively high χ^2 values. The GSAS program provides only the R_F values individually in a coexistence of phases. By comparing the R_F indexes depicted in Table 2, it was verified that the SnO_2 phase presented the highest values, which increased for samples heat treated at higher temperatures. This fact can be attributed to the low resolution of the SnO_2 diffracted peaks due to minor quantity of this phase (mass amount less than 1.5%), prejudicing the fit quality for this phase. On the other hand, low R_F values were obtained for $SrSnO_3$, assuring the fit quality in the perovskite evaluation.

According to literature, different structures are usually observed for $SrSnO_3$ [1–7]. According to Glerup [12], three high temperature structural phase transitions were identified in the perovskite $SrSnO_3$ using differential scanning calorimetry and dilatometry, with subsequent characterization using high-resolution neutron powder diffraction. For synthesis using solid state reaction, $SrSnO_3$ is orthorhombic between 25 and 634 °C, space group *Pmcn,* before undergoing a continuous phase transition to a second orthorhombic phase with space group *Incn*. At 800 °C there is a first order phase transition to a tetragonal phase with space group *I4/mcm* before finally transforming to the aristotype phase at 1,021 °C. All these transitions are presented in Eq. 1.

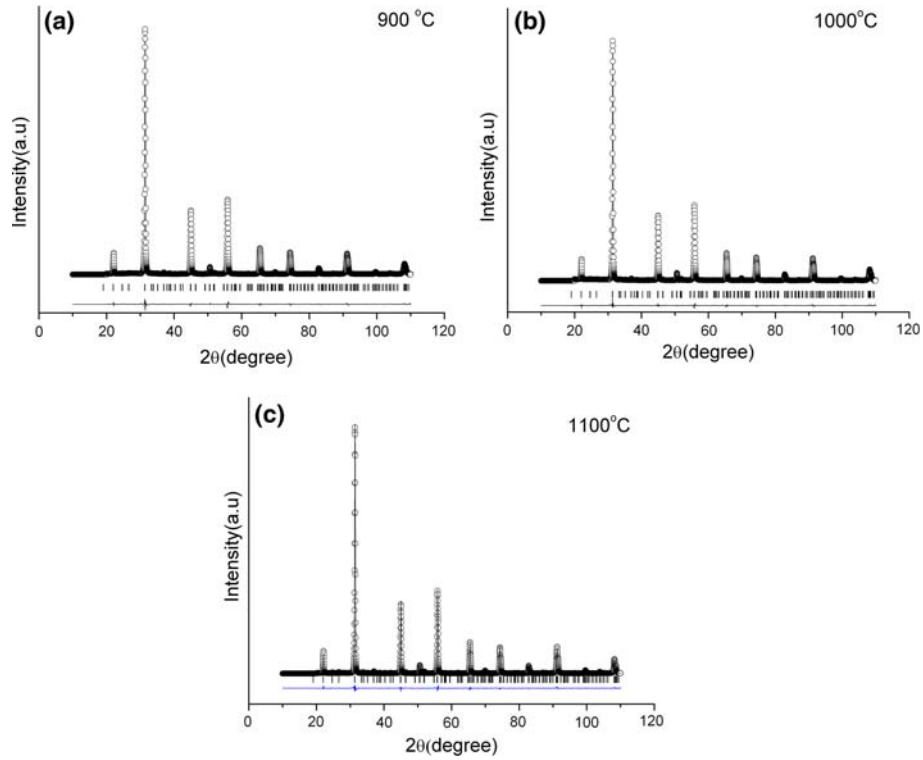

Fig. 4 Observed and calculated XRD patterns using Rietveld refinement of $SrSnO_3$ heat treated at different temperatures: (**a**) 900 °C, (**b**)1000 °C and (**c**) 1100 °C. Legend: | Bragg position; ○ calculated; – observed and – - difference

Table 1 Results of the Rietveld refinement for $SrSnO_3$ (*Pmcn*)

Temp/°C	Lattice parameters/Å^3			Unit cell volume/Å^3	R_{Bragg}/%	R_p /%	RWP/%	CHI^2
	a	*b*	*c*					
900	8.07274	5.71122	5.71251	263.422	1.68	4.47	6.34	2.84
1,000	8.07649	5.70882	5.71109	263.322	1.95	3.92	5.77	2.29
1,100	8.07316	5.71157	5.71157	263.296	1.78	4.48	7.36	3.75

Table 2 Phase amount, in mass percentages

Temperature/°C	$SrSnO_3$/%	RF_{SrSnO3}/%	SnO_2/%	RF_{SnO2}/%
900	98.51	2.19	1.49	3.25
1,000	98.56	2.34	1.44	5.62
1,100	98.64	2.96	1.36	13.57

$$Pmcn \overset{800\ ^\circ C}{\longrightarrow} Incn \overset{900\ ^\circ C}{\longrightarrow} I4/mcm \overset{1{,}000\ ^\circ C}{\longrightarrow} Pm\bar{3}m \quad (1)$$

In the present work, Rietveld refinement indicated that $SrSnO_3$ had an orthorhombic structure with space group *Pmcn* at all heat treatment temperatures. This same space group was reported by Glerup et al. that synthesized $SrSnO_3$ by solid state reaction, but only after calcination at 800 °C [12]. In the present work, the phase transition was not observed. This may be related to the difference in the defect formation when samples are synthesized by solid state reaction or by a soft chemical method.

Typical Rietveld analysis outputs are described in Fig. 4a–c for the quality evaluation of the fitting. It can be observed that the difference between calculated and observed patterns decreased with increasing temperature. This fact was easily visualized at about 31.6°, which corresponded to the mainly reflection of the $SrSnO_3$ phase. This result indicated that an improvement in the orthorhombic crystalline arrangement occurred with increasing calcination temperature.

Small variations were observed on the ***a***, ***b*** and ***c*** lattice parameters; a decrease in cell volume was observed with increasing temperature probably due to the influence of the decrease in the ***c*** parameter.

These results indicated that the endothermic peak at about 1,091 °C in DTA curve (Fig. 1b) was not assigned to a phase transition, being probably related to a structural rearrangement among SnO_6 polyhedra in the orthorhombic perovskite.

Conclusions

$SrSnO_3$ was synthesized by the polymeric precursor method, with orthorhombic structure at all calcination temperatures. TG curves of the powder precursors displayed three thermal decomposition steps, while DTA curves showed six transitions. The elucidation of this behavior was done associating thermal analysis with IR spectroscopy, HTXRD and Rietveld refinement of the XRD patterns of samples calcined between 900 and 1,100 °C. The first step was assigned to the elimination of water and gases adsorbed on powder surface. Infrared spectra confirmed that the second step was assigned to the ester combustion. Evaluation of the third transition was done using infrared spectra and Rietveld refinement, being assigned to the decomposition of strontium carbonate, with two endothermic peaks in the DTA curves. The exothermic peak around 670 °C was determined considering the infrared spectra and HTXRD patterns, being assigned to perovskite crystallization. Rietveld refinement indicated that the last endothermic peak at about 1,091 °C was assigned to a structural rearrangement among SnO_6 polyhedra, not being related to phase transition.

Acknowledgements The authors acknowledge CAPES and CNPq/MCT, PROINFRA/FINEP and CEPID/FAPESP for the financial support.

References

1. Azad AM, Shyan LLW, Yen PT. Synthesis, processing and microstructural characterization of $CaSnO_3$ and $SrSnO_3$ ceramics. J Alloy Compd. 1999;282:109–24.
2. Lu Z, Liu J, Tang J, Li Y. Hydrothermal synthesis of $CaSnO_3$ cubes. Inorg Chem Commun. 2004;7:731–3.
3. Zhang W, Tang J, Ye J. Structural, photocatalytic, and photophysical properties of perovskite $MSnO_3$ (M = Ca, Sr, and Ba) photocatalysts. J Mater Res. 2007;22:1859–71.
4. Mizoguchi H, Eng HW, Woodward PM. Probing the electronic structures of ternary perovskite and pyrochlore oxides containing Sn^{4+} or Sb^{5+}. Inorg Chem. 2004;43:1667–80.
5. Mountstevens EH, Attfield JP, Redfern SAT. Cation-size control of structuralphase transitions in tin perovskitas. J Phys. 2003;15:8315–26.
6. Azad A-M, Hashim M, Baptist S, Badri A, Ul Haq A. Phase evolution and microstructural development in sol-gel derived $MSnO_3$ (M = Ca, Sr and Ba). J Mater Sci. 2000;35:5475–83.
7. Udawatte CP, Kakihana M, Yoshimura M. Low temperature synthesis of pure $SrSnO_3$ and the (Bax Sr_{1-x})SnO_3 solid solution by the polymerized complex method. Solid State Ion. 2000;128:217–26.
8. Alves MCF, Souza SC, Lima SJG, Longo E, Souza AG, Santos IMG. Influence of the precursors salts in the synthesis of $CaSnO_3$ by the polymeric precursor method. J Therm Anal Calorim. 2007;87:763–6.
9. Rietveld HM. A profile refinement method for nuclear and magnetic structures. J Appl Crystallogr. 1969;2:65–71.
10. Larson AC, Von Dreele RB. GSAS-general structure analysis system. Los Alamos National Laboratory, EUA; 2000.
11. Finger LW, Cox LW, Jephcoat DE. A correction for powder diffraction peak asymmetry due to axial divergence. J Appl Crystallogr. 1994;27:892–900.
12. Glerup M, Knight KS, Poulsen FW. High temperature structural phasetransitions in $SrSnO_3$ perovskite. Mater Res Bull. 2005;40:507–20.
13. Nakamoto K. Infrared and Raman spectra of inorganic and coordination compounds. New York: Wiley; 1980.
14. Nyquist R, Kagel R. Infrared spectra of inorganic compounds. London: Academic Press; 1971.
15. Licheron M, Jouarf G, Hussona E. Characterization of $BaSnO_3$, powder obtained by a modified sol-gel route. J Eur Ceram Soc. 1997;17:1453.
16. Vegas A, Vallet-Regý M, González-Calbet JM, Alario-Franco MA. The $ASnO_3$(A=Ca,Sr) perovskites. Acta Crystallogr B. 1986;42:167–72.